

Reactions of Pyrazole with Unsaturated Triangular Clusters of Rhenium. Solid-State and Solution Characterization of an Intramolecular N–H··· π Hydrogen Bond

T. Beringhelli,* G. D'Alfonso,* M. Panigati, and F. Porta

Dipartimento di Chimica Inorganica, Metallorganica e Analitica, e Centro CNR CSMTBO, Via Venezian 21, 20133 Milano, Italy

P. Mercandelli, M. Moret,* and A. Sironi

Dipartimento di Chimica Strutturale e Stereochimica Inorganica, e Centro CNR CSMTBO, Via Venezian 21, 20133 Milano, Italy

Received February 9, 1998

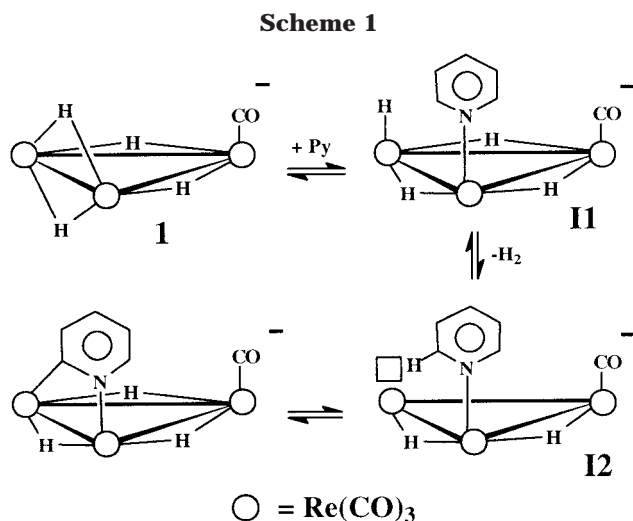
The reaction of the unsaturated anion $[\text{Re}_3(\mu\text{-H})_4(\text{CO})_{10}]^-$ with pyrazole (used as solvent at 80 °C) proceeds in a stepwise manner, at first giving the $[\text{Re}_3(\mu\text{-H})_3(\mu\text{-}\eta^2\text{-pz})(\text{CO})_{10}]^-$ anion (**2**, pz = pyrazolate), with H₂ evolution. Spectroscopic characterization has shown that **2** contains a pz ligand bridging through the two N atoms, one edge of the triangular cluster. At longer times, CO is evolved and **2** transforms into the novel species $[\text{Re}_3(\mu\text{-H})_3(\mu\text{-}\eta^2\text{-pz})(\text{CO})_9(\text{Hpz})]^-$ (**3**), containing one pz ligand bridging a cluster edge and a second pyrazole molecule terminally bonded on the third vertex of the triangle, replacing an axial carbonyl of **2**. The treatment with CO (atmospheric pressure, room temperature) slowly restores **2**. A single-crystal X-ray analysis of **3** has revealed the syn coordination of the two heterocycles with respect to the metal triangle plane and an intramolecular hydrogen bond between the N–H proton of the pyrazole ligand and the aromatic π -electrons of the bridging pyrazolate. There is NMR evidence that this intramolecular hydrogen bond is maintained in CD₂Cl₂ solution: (i) the N–H protonic resonance is significantly shifted upfield, with respect to the values typical of complexes containing Hpz, due to the screening effect of the π -electron cloud; (ii) a 2D NOESY experiment has shown a dipolar interaction between H _{α} of the pyrazolate and the N–H protonic resonance (and, to a lesser extent, H _{α} of the pyrazole). In acetone, intermolecular N–H···solvent interactions replace, in part, the intramolecular H bond and different conformers are populated in different ratios on varying the temperature, as shown by variable-temperature and nOe (1D and 2D) experiments. Further reacting **1** in molten pyrazole causes fragmentation of the triangular cluster moiety with formation of the novel dinuclear anion $[\text{Re}_2(\mu\text{-H})(\mu\text{-}\eta^2\text{-pz})_2(\text{CO})_6]^-$ (**4**) and of the neutral complex $[\text{Re}(\text{pz})(\text{CO})_3(\text{Hpz})_2]$. A single-crystal X-ray analysis of the $[\text{NEt}_4]^+$ salt of **4** showed that the dinuclear anion contains two *fac*-Re(CO)₃ units linked by one hydrido and two pyrazolato bridging ligands, with the two $\mu\text{-}\eta^2\text{-pz}$ units almost orthogonal to each other. A more selective route to anion **3** is provided by the reaction of the 46 valence electron complex $[\text{Re}_3(\mu\text{-H})_4(\text{CO})_9(\text{Hpz})]^-$ (**6**) with Hpz. On using pyrazole deuterated in the nitrogen site, HD evolution has been demonstrated. The treatment of **6** with MeCN affords, even if very slowly, another derivative containing a bridging pyrazolate, namely the anion $[\text{Re}_3(\mu\text{-H})_3(\mu\text{-}\eta^2\text{-pz})(\text{CO})_9(\text{NCMe})]^-$, characterized spectroscopically. Also, the unsaturated anion $[\text{Re}_3(\mu\text{-H})_4(\text{CO})_9(\text{PMe}_2\text{Ph})]^-$ reacts with Hpz, giving two isomers of the $[\text{Re}_3(\mu\text{-H})_3(\mu\text{-}\eta^2\text{-pz})(\text{CO})_9(\text{PMe}_2\text{Ph})]^-$ anion (with the phosphine in an axial and equatorial position, respectively). The reactions rates of the 46 valence electron complexes $[\text{Re}_3(\mu\text{-H})_4(\text{CO})_9\text{L}]^-$ with pyrazole increase on increasing the electron density on the cluster (in the order L = Hpz > PMe₂Ph > CO), suggesting that the rate is controlled by the interaction of a “hydridic” H ligand with the acidic N–H bond of pyrazole. In no case has activation of the ortho C–H bond of pyrazole been observed.

Introduction

It has been previously shown that the unsaturated triangular cluster anion $[\text{Re}_3(\mu\text{-H})_4(\text{CO})_{10}]^-$ (**1**, 46 valence electrons) is able to activate the ortho C–H bond of pyridine, giving a derivative containing an ortho-metalated pyridine moiety.¹ Regioselective H/D ex-

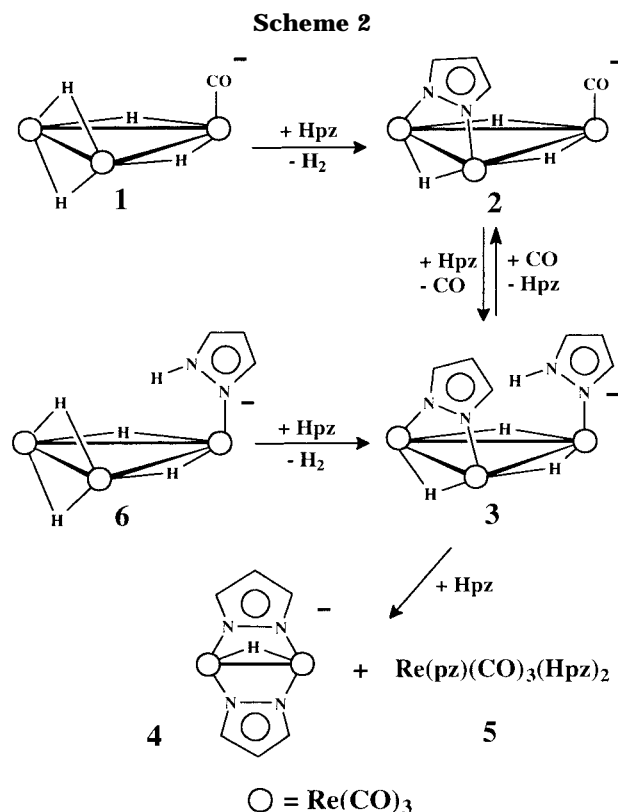
change processes between the hydrides and the ortho position of the pyridine revealed the reversibility of the C–H oxidative addition. Moreover, under high H₂ pressure it was possible to expel the pyridine ligand

(1) Beringhelli, T.; Ciani, G.; D'Alfonso, G.; Proserpio, D. M.; Sironi, A. *Organometallics* **1993**, *12*, 4863.



from the cluster, restoring the unsaturated starting anion **1**.² On using deuterated pyridine, evidence was obtained supporting the mechanism shown in Scheme 1, involving pyridine coordination and subsequent reductive elimination of two H ligands, affording the coordinatively unsaturated species **I2**. This key intermediate was also formed by the C–H reductive elimination in the reverse step; therefore, the competition between intramolecular C–H oxidative addition and coordination of a different ligand, such as CO, could be studied starting either from the unsaturated anion **1** or from the saturated orthometalated derivative [Re₃(μ-H)₃(μ-η²-NC₅H₄)(CO)₁₀]⁻.²

Due to continuing interest in the reactivity of aromatic nitrogen heterocycles with transition metals, in particular for the activation of C–H and N–H bonds in these molecules,³ we decided to investigate the reactions of **1** with a different heterocycle, such as pyrazole. Despite being a poor base,⁴ pyrazole is a good σ-donor, acting as a monodentate ligand through its pyridinic nitrogen atom, or as a bidentate bridging ligand in the form of the pyrazolato anion.^{5,6} In our system, the coordination of pyrazole would give an intermediate similar to **II** of Scheme 1, offering the chance to study the competition between C–H or N–H activation on the Re cluster. In the related reaction of pyrazole with the Os₃(CO)₁₀ fragment, it has been previously shown^{3c,7} that the products of activation of the N–H and C_α–H bonds are formed, with the first one dominating.



Results and Discussion

Stepwise Reaction of **1 in Molten Pyrazole.** The reactivity of **1** with pyrazole has been studied using the ligand itself as solvent, carrying out the reactions at a temperature just above the melting point of pyrazole (70 °C). In these conditions, mixtures of the four species [Re₃(μ-H)₃(μ-η²-pz)(CO)₁₀]⁻ (**2**), [Re₃(μ-H)₃(μ-η²-pz)(CO)₉(Hpz)]⁻ (**3**), [Re₂(μ-H)(μ-η²-pz)₂(CO)₆]⁻ (**4**), and [Re(pz)(CO)₃(Hpz)₂] (**5**) described below are formed.

Attempts to improve the selectivity on performing the reaction in THF, at lower temperatures, were unsuccessful. At room temperature, no reaction was observed after 24 h upon addition of 50 equiv of pyrazole to a THF solution of **1**. On increasing both temperature (40 °C) and pyrazole (700 equiv), complete disappearance of **1** occurred after 24 h but spectroscopic monitoring showed the formation of a mixture containing all of the species **2–5**. No improvement of selectivity was obtained on lowering the amount of pyrazole.

However, the selectivity of the reaction in molten pyrazole could be partially controlled by a careful choice of the reaction time. When the reaction was stopped after a very short time (2 min after the complete dissolution of [NEt₄]**1**), the main reaction product (>90%) was spectroscopically identified as the [Re₃(μ-H)₃(μ-η²-pz)(CO)₁₀]⁻ anion (**2**, pz = pyrazolate) of Scheme 2. The presence of the pyrazolate ligand bridging one edge of the triangular cluster is indicated by the two resonances, in a 1:2 ratio, in the region of the aromatic protons. The C_s symmetry imposed to the anion by the N,N-exo-bidentate coordination of pz is confirmed by the presence of two hydridic resonances, in a 1:2 ratio, down to 193 K. The δ values of the hydridic signals (–11.56 and –13.59 ppm, 1:2, acetone-*d*₆) show the

(2) Beringhelli, T.; Carlucci, L.; D'Alfonso, G.; Ciani, G.; Proserpio, D. M. *J. Organomet. Chem.* **1995**, *504*, 15.

(3) See for instance: (a) Garcia, E.; Kolwaite, D. S.; Rosenberg, E.; Hardcastle, K.; Ciurash, J.; Duque, R.; Gobetto, R.; Milone, L.; Osella, D.; Botta, M.; Dastrù, W.; Viale, A.; Fiedler, I. *Organometallics* **1988**, *17*, 415. (b) Kabir, S. E.; Kolwaite, D. S.; Rosenberg, E.; Hardcastle, K.; Cresswell, W.; Grindstaff, J. *Organometallics* **1995**, *14*, 3611. (c) Agarwala, R.; Azam, K. A.; Dilshad, R.; Kabir, S. E.; Miah, R.; Shahiduzzaman, M.; Hardcastle, K. I.; Rosenberg, E.; Hursthouse, M. B.; Malik, K. M. A. *J. Organomet. Chem.* **1995**, *492*, 135 and references therein.

(4) (a) Reedijk, J. In *Comprehensive Coordination Chemistry*; Wilkinson, G., Ed.; Pergamon Press: New York, 1987; Vol. 2, p 73. (b) Catalan, J.; Abboud, J. L. M.; Elguero, J. *Adv. Heterocycl. Chem.* **1987**, *41*, 187.

(5) La Monica, G.; Ardizzoia, G. A. *Prog. Inorg. Chem.* **1997**, *46*, 151 and references therein.

(6) Sadimenko, A. P.; Basson, S. S. *Coord. Chem. Rev.* **1996**, *147*, 247 and references therein.

(7) Shapley, J. R.; Samkoff, D. E.; Bueno, C.; Churchill, M. R. *Inorg. Chem.* **1982**, *21*, 634.

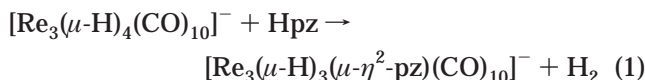
Table 1. Variable-Temperature ^1H HMR Data for the Pyrazole Ligand^a in $[\text{NEt}_4]\mathbf{3a}$ (ca. 0.035 M)^b

T (K)	CD_2Cl_2				acetone- d_6			
	N–H	H α	H γ	H β	N–H	H α	H γ	H β
193	7.12	6.89	7.68	6.13	12.19	7.64	6.61	6.07
213					11.71	7.54	6.84	6.05
233					11.30	7.47	6.98	6.04
253					10.95	7.41	7.08	6.04
273					10.61	7.35	7.17	6.04
298	7.78	6.91	7.68	6.11	10.25	7.30	7.25	6.04

^a The bridging pyrazolate gives resonances at 7.31 (H α), 6.03 (H β) ppm [CD_2Cl_2 , 298 K]; 7.23 (H α), 5.97 (H β) ppm [CD_2Cl_2 , 193 K]; 7.06 (H α), 5.74 (H β) ppm [acetone- d_6 , 298 K]; 7.00 (H α), 5.64 (H β) ppm [acetone- d_6 , 193 K]. ^b Free pyrazole: (0.024 M) CD_2Cl_2 , 193 K 12.53 (1), 7.74 (2), 6.39 (1) ppm; 298 K 9.63 (1), 7.60 (2), 6.40 (1) ppm; acetone- d_6 (0.28 M) 193 K 12.94 (1), 7.84 (1, br), 7.69 (1, br), 6.37 (1) ppm; 298 K 12.13 (1), 7.61 (2), 6.28 (1) ppm. In the latter solvent, the resonances of the pyrazole–acetone adduct are also observed, as previously reported (Nesmeyanov, A. N.; Zavelovich, E. B.; Babin, V. N.; Kochetkova, N. S.; Fedin, E. I. *Tetrahedron* **1975**, *31*, 1463).

usual low-field shift caused by N-donor ligands, with respect to the value of ca. –17 ppm typical of bridging hydrides in saturated clusters of rhenium containing carbonyl ligands only.^{8,9}

The reaction occurs with H_2 evolution, as indicated by gas chromatographic analysis, according to eq 1.



Differently from what was observed in the case of pyridine, the reaction is not reversible, even under high H_2 pressure (see Experimental Section).

The evolved H_2 could arise by interaction of a hydride with the N–H proton or by reductive elimination of two hydrides, as shown in Scheme 1 for the reaction with pyridine. In this case, the mechanism reported in Scheme 1 was proved by showing that deuterated pyridine gives an orthometalated derivative containing two H and one D atoms in the hydridic sites. We, therefore, tried to study reaction 1 with pyrazole selectively deuterated in the nitrogen site to verify the fate of the D atom (evolved as HD or bonded to the cluster in a “ $\text{Re}_3\text{H}_2\text{D}$ ” isotopomer). However, ^1H and ^2H NMR analyses of samples taken at different reaction times showed extensive deuteration of the hydridic sites of the parent anion **1** itself, thus preventing any mechanistic inference.

When the reaction of **1** with molten pyrazole was carried out for longer reaction times, the concentration of **2** slowly decreased (with a $t_{1/2}$ of ca. 70 min, see Experimental Section) and two novel hydridic species **3** and **4** were formed.

Compound **3** has been formulated, on the basis of its NMR data (see Experimental Section and Table 1), as the anion $[\text{Re}_3(\mu\text{-H})_3(\mu\text{-}\eta^2\text{-pz})(\text{CO})_9(\text{Hpz})]^-$ containing one pyrazolato ligand bridging a cluster edge and a second pyrazole molecule terminally bonded on the third vertex of the triangle, replacing an axial carbonyl of **2** (see Scheme 2). The two hydridic resonances (δ –9.90

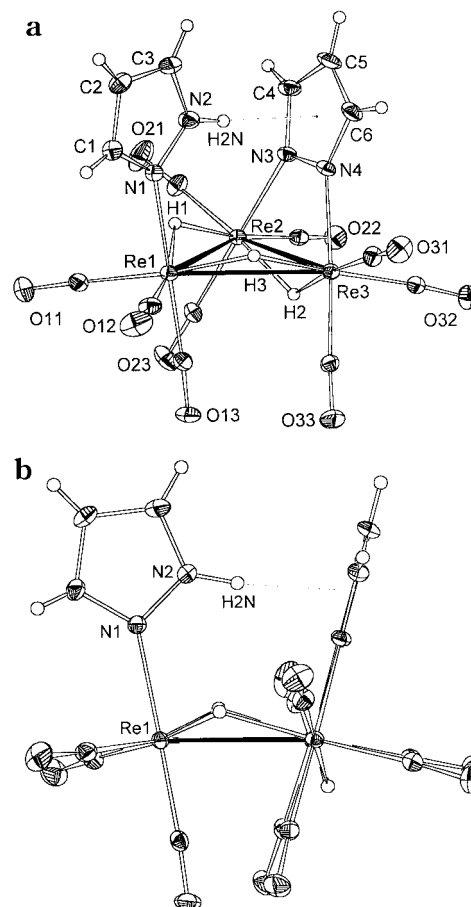
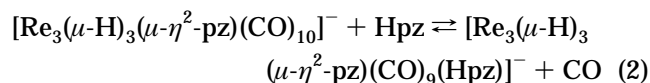


Figure 1. ORTEP drawing of the $[\text{Re}_3(\mu\text{-H})_3(\mu\text{-}\eta^2\text{-pz})(\text{CO})_9(\text{Hpz})]^-$ anion (**3a**) with partial labeling scheme. Thermal ellipsoids drawn at the 30% probability level. Hydrogen atoms were given arbitrary radii. (1a) Perspective view with the N–H $\cdots\pi$ hydrogen bond and (1b) lateral view to emphasize the coordination octahedra tilting.

and –11.29 ppm, in a 2:1 ratio, in CD_2Cl_2 at 298 K) show that **3** maintains the C_s symmetry of **2**. This implies either free rotation of the Hpz ligand or freezing of a rotamer with the ligand plane lying on the idealized mirror. This point will be discussed later. The chemical shift of the hydride bridging the $\text{Re}(\mu\text{-pz})\text{Re}$ interaction is substantially unchanged with respect to **2**, while the hydrides bridging the lateral edges show the low-field shift expected for the replacement of a carbonyl by the N-donor ligand. A single-crystal X-ray analysis was performed to establish the syn or anti coordination of the two aromatic rings with respect to the cluster plane. The structure of the syn configuration is depicted in Figure 1 and will be described in detail in the following discussion.

The formation of **3** clearly arises from the thermal lability of an axial carbonyl of the $\text{Re}(\text{CO})_4$ vertex of **2** (eq 2). Also, the reaction of **1** with pyridine gives



(8) Beringhelli, T.; D'Alfonso, G.; Freni, M.; Ciani, G.; Sironi, A.; Molinari, H. *J. Chem. Soc., Dalton Trans.* **1986**, 2691.

(9) Beringhelli, T.; D'Alfonso, G.; Panigati, M. *J. Organomet. Chem.* **1997**, *527*, 215.

an analogous $[\text{Re}_3(\mu\text{-H})_3(\mu\text{-}\eta^2\text{-NC}_5\text{H}_4)(\text{CO})_9(\text{NC}_5\text{H}_5)]^-$ derivative when performed at high temperature (80 °C).

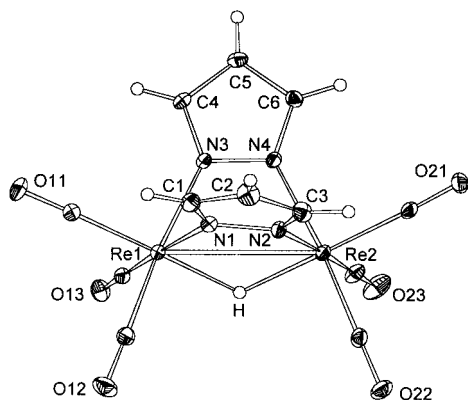
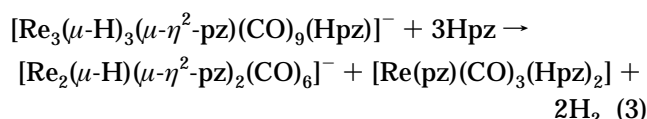


Figure 2. ORTEP drawing of the $[\text{Re}_2(\mu\text{-H})(\mu\text{-}\eta^2\text{-pz})_2(\text{CO})_6]^-$ anion (**4**) with partial labeling scheme. Thermal ellipsoids drawn at the 30% probability level. Hydrogen atoms were given arbitrary radii.

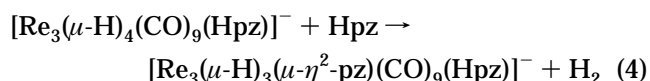
Reaction 2 is reversible: treatment with CO (1 atm) results in the transformation of **3** into **2**, but the reaction is very slow (complete after 1 week, at room temperature).

The third hydridic species observed in the reaction mixtures in molten pyrazole (**4**) shows one hydridic and two pyrazolic resonances in the ^1H NMR spectrum (ratio 1:2:4). A single-crystal X-ray analysis formulated this novel product as the dinuclear anion $[\text{Re}_2(\mu\text{-H})(\mu\text{-}\eta^2\text{-pz})_2(\text{CO})_6]^-$ containing two pyrazolato and one hydrido ligand bridging the Re–Re interaction (see Figure 2 and the description of the structure below).

A fourth product has been recognized in the hexane solution used to separate the NET_4^+ salts of the anionic products from the excess of pyrazole (see Experimental Section). On the basis of its IR and NMR data, it has been formulated as the neutral mononuclear complex $[\text{Re}(\text{pz})(\text{CO})_3(\text{Hpz})_2]$ (**5**), recently synthesized and characterized.¹⁰ Equation 3 formally accounts for the fragmentation of the trinuclear cluster **3** to **4** and **5**.



Reactivity of other $[\text{Re}_3(\mu\text{-H})_4(\text{CO})_9\text{L}]^-$ Unsaturated Anions. A more selective route to anion **3** is provided by reaction 4, whose starting material is the unsaturated anion $[\text{Re}_3(\mu\text{-H})_4(\text{CO})_9(\text{Hpz})]^-$ (**6**, 46 valence electrons) containing a pyrazole ligand terminally bonded on a vertex of the triangle (see Scheme 2).¹¹ Reactions



1 and 4 are fully analogous, because both involve the formation of a bridging pyrazolato ligand, with H_2 evolution, from the reaction of Hpz with a 46-valence electron complex. However reaction 4 occurs in much milder conditions than reaction 1. Indeed, in CH_2Cl_2

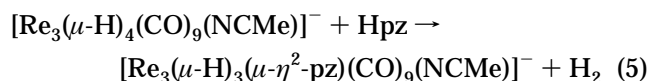
solution, it goes to completion in ca. 3 h, at room temperature, in the presence of only 10 equiv of pyrazole.

NMR monitoring of reaction 4 showed, at the beginning of the experiment, the formation of a novel species besides anion **3**, responsible for two hydridic resonances at $\delta -10.80$ and -11.82 ppm, in 2:1 ratio. This species can be reasonably formulated as an isomer of anion **3**, containing the two pyrazole rings in an anti configuration (**3b**). At the initial stages of the reaction, **3b** is formed in a comparable amount with the syn isomer (hereafter referred to as **3a**). Its concentration attains the maximum value (10–15%) at about one-half of the reaction time, then slowly decreases, leaving **3a** as the unique final product (see Figure S1 in the Supporting Information). Mixtures of syn and anti isomers have also been obtained in the reactions of the μ_3 -imidoyl cluster $[\text{Os}_3(\mu\text{-H})(\mu_3\text{-}\eta^2\text{-C}=\text{NC}_3\text{H}_6)(\text{CO})_9]$ with amines.¹² In this case, it was shown that the syn isomer was the kinetic product while the thermodynamically favored species depended on the cone angle of the amine, the bulkier ligands (such as pyrrolidine) slightly favoring the isomer containing the μ -imidoyl and the amine on the same face of the cluster.

In the case of reaction 4, it was possible to perform experiments with selectively deuterated pyrazole, because the milder reaction conditions, with respect to reaction 1, prevented deuteration of the hydridic sites of the starting complex. NMR monitoring of the reaction of **6** with D-pz clearly showed the appearance of the pseudotriplet (δ 4.4 ppm, $J_{\text{HD}} = 43$ Hz) due to free HD, thus demonstrating that H_2 evolved in reaction 4 arises from one hydride and the N–H proton and not from two H ligands. It was not possible to establish if the D atom came from free or coordinated pyrazole, because the easy intermolecular exchange of the protons on nitrogen did not allow the selective isotopic labeling of the NH sites.

Other experiments were then designed to differentiate the two “roles” of Hpz in reaction 4 (coordinated or entering ligands). With this aim, we pursued the synthesis of $[\text{Re}_3(\mu\text{-H})_3(\mu\text{-}\eta^2\text{-pz})(\text{CO})_9\text{L}]^-$ derivatives, containing L ligands different from CO or Hpz, through two different ways: (i) reaction of $[\text{Re}_3(\mu\text{-H})_4(\text{CO})_9(\text{Hpz})]^-$ with L; (ii) reaction of $[\text{Re}_3(\mu\text{-H})_4(\text{CO})_9\text{L}]^-$ complexes with Hpz.

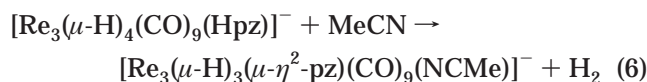
The first route proved to be impracticable with good L ligands such as CO or PMe_2Ph , because they rapidly substituted the pyrazole ligand. With the poor ligand MeCN (used in a 10-fold excess) the slow formation of the expected $[\text{Re}_3(\mu\text{-H})_3(\mu\text{-}\eta^2\text{-pz})(\text{CO})_9(\text{NCMe})]^-$ anion (**7**) was observed (see Experimental Section), but also accompanied, in this case, by a significant amount of the substitution derivative $[\text{Re}_3(\mu\text{-H})_4(\text{CO})_9(\text{NCMe})]^-$ (**8**). The presence of **8**, able to give **7** by reaction with Hpz (eq 5), does not permit us to say with certainty that **7** derives from reaction 6. However, the concentration of



(10) Ardizzoia, A. G.; La Monica, G.; Maspero, A.; Moret, M.; Masciocchi, N. *Eur. J. Inorg. Chem.*, in press.

(11) Beringhelli, T.; D'Alfonso, G.; Panigati, M.; Porta, F.; Mercantelli, P.; Moret, M.; Sironi, A. Manuscript in preparation.

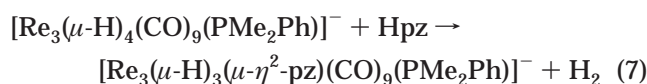
(12) Kabir, S. E.; Rosenberg, E.; Day, M.; Hardcastle, K.; Wolf, E.; McPhillips, T. *Organometallics* **1995**, *14*, 721.



free pyrazole present in the reaction mixture must be considered very low, the upper limit being the amount of **8**. This is confirmed by the very small amount of **3** simultaneously formed by reaction of **6** with Hpz (see Experimental Section). Moreover, the time course of the formation of **7** shows the absence of the "induction period", which is typical of consecutive reactions. We can, therefore, be confident that reaction 6 does occur.

The nature of anion **7** has been established from its ¹H NMR data: the two hydridic resonances, in a 1:2 ratio, are at δ values in line with the presence of three coordinated N atoms (−10.79 and −11.66 ppm, 2:1, CD₂-Cl₂). The two signals of the pyrazolate (2:1 ratio) confirm the C_s symmetry of the anion, while the resonance of MeCN (δ 1.78 ppm) appears upfield with respect to the free ligand. This could be attributable to the shielding effect of the π -electron cloud of the bridging pyrazolate, as previously observed for the dominant isomer of the related [Re₃(μ -H)₃(μ - η^2 -NC₅H₄)(CO)₉(NCMe)][−] anion.⁹ On these grounds, **7** should be identified as the syn isomer. There is no evidence for the presence of an anti isomer, though it could be responsible of some of the very minor signals observed in the reaction mixture.

As to the second route to [Re₃(μ -H)₃(μ - η^2 -pz)(CO)₉L][−] anions, the fast substitution of pyridine with pyrazole made impossible the use of [Re₃(μ -H)₄(CO)₉(Py)][−], which could be a very good model of the anion **6**. Thus, we moved to the unsaturated complex [Re₃(μ -H)₄(CO)₉(PMe₂-Ph)][−] that contains a less labile, but still good σ -donor ligand. In this case, the clean formation of two isomers of the mixed pyrazolato-phosphine derivative [Re₃(μ -H)₃(μ - η^2 -pz)(CO)₉(PMe₂Ph)][−] (**9**) was observed. The two species, assigned on the basis of the pattern of the hydridic resonances to an axial (**9a**) and equatorial (**9b**) isomer, respectively, are always in ca. 4:1 ratio, which likely represents their thermodynamic ratio. In fact, the rate of reaction 7 was low, much lower than that of reaction 4 (ca. 40% of conversion after 24 h, in the same conditions of reaction 4, i.e., in CD₂Cl₂, at 298 K, in the presence of 10 equiv of pyrazole), but faster than reaction 1 in the same conditions (no reaction after 24 h).



Description of the Structures of Anions 3a and 4. Crystals of the PPh₄⁺ salt of anion **3a** consist of the packing of discrete anions and cations plus clathrated CH₂Cl₂ molecules in a 1:1:1 ratio, respectively, held together by Coulombic and van der Waals interactions. An ORTEP drawing of the molecular structure of **3a** is reported in Figure 1. Relevant bond parameters are listed in Table 3.

Anion **3a** possesses a triangular metal core with all edges bridged by one hydrido ligand. Each of the rhenium atoms also bears three terminal CO ligands with facial coordination. With reference to the parent

Table 2. Summary of Crystal Data and Structure Refinement Parameters for 3a and 4

	3a	4
formula	C ₄₀ H ₃₂ Cl ₂ N ₄ O ₉ PRE ₃	C _{36.5} H ₂₈ ClN ₄ O ₆ PRE ₂
fw	1373.17	1057.45
cryst syst	triclinic	monoclinic
space group	P $\bar{1}$ (No. 2)	C2/c (No. 15)
a, Å	9.239(1)	37.584(1)
b, Å	14.050(2)	10.102(1)
c, Å	17.688(2)	21.536(2)
α , deg	91.49(6)	
β , deg	91.56(2)	114.03(1)
γ , deg	103.85(5)	
V, Å ³	2227.2(5)	7468(1)
Z	2	8
temp, K	223(2)	223(2)
abs coeff, mm ^{−1}	8.344	6.642
no. indep reflns,	9474, 0.0241	8308, 0.0279
<i>R</i> (int)		
R1, wR2 (<i>F</i> _o >	0.0197, 0.0382	0.0210, 0.0391
4 σ (<i>F</i> _o) ^a		
R1, wR2 (all data)	0.0280, 0.0393	0.0331, 0.0415

Table 3. Selected Bond Distances (Å) and Angles (deg) for 3a and 4

	3a	4	
Re(1)–Re(2)	3.259(1)	Re(1)–Re(2)	3.2380(2)
Re(1)–Re(3)	3.277(1)	Re(1)–C(11)	1.921(3)
Re(2)–Re(3)	3.217(1)	Re(1)–C(12)	1.926(3)
Re(1)–C(11)	1.905(4)	Re(1)–C(13)	1.923(3)
Re(1)–C(12)	1.913(4)	Re(2)–C(21)	1.925(3)
Re(1)–C(13)	1.924(4)	Re(2)–C(22)	1.923(3)
Re(2)–C(21)	1.919(4)	Re(2)–C(23)	1.929(4)
Re(2)–C(22)	1.922(4)	Re(1)–N(1)	2.166(2)
Re(2)–C(23)	1.908(4)	Re(2)–N(2)	2.163(2)
Re(3)–C(31)	1.908(4)	Re(1)–N(3)	2.156(2)
Re(3)–C(32)	1.914(4)	Re(2)–N(4)	2.170(2)
Re(3)–C(33)	1.913(4)		
Re(1)–N(1)	2.209(3)		
Re(2)–N(3)	2.161(3)		
Re(3)–N(4)	2.175(3)		
Re(1)–Re(2)–Re(3)	60.79(2)	C(11)–Re(1)–C(12)	89.8(1)
Re(1)–Re(3)–Re(2)	60.24(4)	C(11)–Re(1)–C(13)	89.6(1)
Re(2)–Re(1)–Re(3)	58.97(3)	C(12)–Re(1)–C(13)	89.4(1)
C(11)–Re(1)–C(12)	90.8(2)	C(11)–Re(1)–N(3)	95.2(1)
C(11)–Re(1)–C(13)	87.6(2)	C(12)–Re(1)–N(3)	174.0(1)
C(12)–Re(1)–C(13)	89.8(2)	C(13)–Re(1)–N(3)	94.0(1)
C(11)–Re(1)–N(1)	93.3(2)	C(11)–Re(1)–N(1)	96.0(1)
C(12)–Re(1)–N(1)	88.6(1)	C(12)–Re(1)–N(1)	94.41
C(13)–Re(1)–N(1)	178.2(1)	C(13)–Re(1)–N(1)	173.3(1)
C(21)–Re(2)–C(22)	89.4(2)	N(1)–Re(1)–N(3)	81.77(8)
C(21)–Re(2)–C(23)	87.4(2)	C(21)–Re(2)–C(22)	90.7(1)
C(22)–Re(2)–C(23)	91.6(2)	C(21)–Re(2)–C(23)	89.7(1)
C(21)–Re(2)–N(3)	95.3(2)	C(22)–Re(2)–C(23)	87.1(1)
C(22)–Re(2)–N(3)	91.8(1)	C(21)–Re(2)–N(2)	94.6(1)
C(23)–Re(2)–N(3)	175.7(1)	C(22)–Re(2)–N(2)	94.9(1)
C(31)–Re(3)–C(32)	89.8(2)	C(23)–Re(2)–N(2)	175.2(1)
C(31)–Re(3)–C(33)	88.9(2)	C(21)–Re(2)–N(4)	93.7(1)
C(32)–Re(3)–C(33)	87.5(2)	C(22)–Re(2)–N(4)	175.1(1)
C(31)–Re(3)–N(4)	94.7(2)	C(23)–Re(2)–N(4)	94.9(1)
C(32)–Re(3)–N(4)	94.2(1)	N(2)–Re(2)–N(4)	82.69(8)
C(33)–Re(3)–N(4)	176.0(1)		

cluster [Re₃(μ -H)₄(CO)₁₀][−],¹³ one axial CO of the Re(CO)₄ unit is actually replaced by a monodentate N-coordinated pyrazole while the Re–Re edge originally bridged by two hydrides is now spanned by a hydride and a μ - η^2 -pyrazolato group, acting as an exo-bidentate ligand. When considering the bonding interactions around the Re atoms, each metal attains a distorted octahedral coordination given by three CO's, two hydrides, and one

(13) Beringhelli, T.; Ciani, G.; D'Alfonso, G.; Molinari, H.; Sironi, A. *Inorg. Chem.* **1985**, *24*, 2666.

nitrogen atom, if direct metal–metal interactions are neglected. Cluster **3a** shows two long Re–Re distances (Re(1)–Re(2) 3.259(1) Å and Re(1)–Re(3) 3.277(1) Å) and one shorter interaction (Re(2)–Re(3) 3.217(1) Å) bridged by the pyrazolato ligand; a similar pattern has been observed in the related $[\text{Re}_3(\mu\text{-H})_3(\mu\text{-}\eta^2\text{-NC}_5\text{H}_4)(\text{CO})_9(\text{NC}_5\text{H}_5)]^-$ ($\text{NC}_5\text{H}_5 = \text{pyridine}$) cluster¹ where pyridine substitutes for pyrazole. Compared to $[\text{Re}_3(\mu\text{-H})_4(\text{CO})_{10}]^-$, the metal framework in **3a** is enlarged significantly; the most evident distance expansion, involving Re(2)–Re(3) increasing from 2.789(1) to 3.217(1) Å, is due to the removal of the formal double Re–Re bond, while the remaining two edges, which are enlarged by about 0.08 Å, suffer from the steric presence of the pyrazole pointing toward the $\mu\text{-}\eta^2$ -pyrazolate. As anticipated in the previous sections, the two pyrazole moieties lie on the same side of the Re_3 triangle giving rise to a syn conformation and are involved in a $\text{N-H}\cdots\pi$ -electrons hydrogen bond. The two pyrazolic rings are almost orthogonal to each other (dihedral angle 83.4(2)°), in accordance with a significant interaction between the N(2)–H(2N) group, the π -electron cloud of the pyrazolato ligand, and an overall C_s idealized symmetry (in the related $[\text{Re}_3(\mu\text{-H})_3(\mu\text{-}\eta^2\text{-NC}_5\text{H}_4)(\text{CO})_9(\text{NC}_5\text{H}_5)]^-$ anion the two heterocyclic ligands are syn but face each other in an almost parallel fashion).¹ H(2N) to $\mu\text{-pz}$ distances range from about 2.22 and 2.36 Å for N(3) and N(4), respectively, to 2.40, 2.61, and 2.64 Å for C(4), C(6), and C(5), respectively, with a H(2N)–pz(centroid) distance of 2.15 Å and a N(2)–H(2N)–pz(centroid) angle of 165°. Recently,¹⁴ intermolecular $\text{N-H}\cdots\pi$ hydrogen-bonded systems have received attention owing to their relevant contribution to crystal packing motives. In such systems, the average distance between H and the π -cloud centroid is about 2.45 Å, suggesting that the $\text{N-H}\cdots\pi$ intramolecular interaction in **3a** is strong enough to stabilize the orthogonal versus the parallel¹ conformation of the aromatic ligands and to offer further reasons for the preference for the syn versus the anti isomer.

Hydrides H(1) and H(3) are displaced about 0.5 Å off the metal triangle on the same side of the pyrazole moieties, while the hydride H(2) lies opposite $\mu\text{-pz}$, about 0.9 Å off the metal plane. Owing to the presence of the intramolecular hydrogen bond involving the two heterocycles, which imposes their orthogonal conformation, the coordination octahedra at the Re atoms are significantly tilted with respect to the Re_3 plane, as outlined in Figure 1b and by the values of the angle between the Re_3 plane, the Re(1)–N(1) vector (100.74(8)°), and the bridging pyrazolate (105.0(1)°). On the contrary, in $[\text{Re}_3(\mu\text{-H})_3(\mu\text{-}\eta^2\text{-NC}_5\text{H}_4)(\text{CO})_9(\text{NC}_5\text{H}_5)]^-$, owing to the parallel conformation of the heterocyclic ligands and the consequent decrease of the steric crowding, the average Re–Re–N(terminal) angles amount to 94.0° (99.3° in **3a**) and the $\text{Re}_3/\mu\text{-NC}_5\text{H}_4$ dihedral angle is 93.5°. Re–N bond lengths in **3a** are normal and show increased values for the axial pyrazole (Re(1)–N(1) = 2.209(3) Å) with respect to the bridging pyrazolato unit (Re(2)–N(3) = 2.161(3) Å, Re(3)–N(4) = 2.175(3) Å).

Crystals of **4** consist of the packing of $[\text{Re}_2(\mu\text{-H})(\mu\text{-}\eta^2\text{-pz})_2(\text{CO})_6]^-$ anions and PPh_4^+ cations together with clathrated CH_2Cl_2 molecules in a 1:1:0.5 ratio, respectively. The molecular structure of **4** is shown in Figure 2, together with a partial labeling scheme. The dinuclear anion contains two *fac*- $\text{Re}(\text{CO})_3$ units linked by one hydrido and two pyrazolato bridging ligands (34 valence electrons), giving rise to a distorted octahedral coordination around the Re centers. The two $\mu\text{-}\eta^2\text{-pz}$ units are almost orthogonal to each other (dihedral angle between least-squares planes 89.3(1)°) with the Re–[N–N]₂–Re metallacycle adopting a boat conformation, giving a C_{2v} idealized symmetry for this dimeric species.

Dimeric rhenium(I) compounds bridged by pyrazolate are a novel class of compounds, the only other examples known being the 36-valence electron compounds $[\text{Re}_2(\mu\text{-X})(\mu\text{-}\eta^2\text{-pz})_2(\text{CO})_6]^-$ (X = OH, Br).¹⁰ In the past, pyrazolato ligands coordinating in an exo-bidentate mode¹⁵ have shown a great coordination versatility regarding the spanned metal–metal distance, the N–N–metal bond angles, and the off-plane displacement of the coordinated metals. In the present case, the Re–Re distance of 3.2380(2) Å is comparable to that observed in the dimeric 34-valence electron compounds with a bridging orthometalated pyridine $[\text{Re}_2(\mu\text{-H})(\mu\text{-}\eta^2\text{-C}_5\text{NH}_4)(\text{CO})_7\text{L}]$ (L = CO, $(\text{CH}_3)_3\text{NO}$),¹⁶ which exhibit values ranging from 3.195 to 3.232 Å. On the contrary, the 36-valence electron compounds $[\text{Re}_2(\mu\text{-OH})(\mu\text{-}\eta^2\text{-pz})_2(\text{CO})_6]^-$ and $[\text{Re}_2(\mu\text{-Br})(\mu\text{-}\eta^2\text{-pz})_2(\text{CO})_6]^-$ have Re···Re distances of 3.660(1) and 3.825(1) Å,¹⁰ respectively, as expected well beyond the accepted range of bond interactions. To alleviate these relevant variations in the Re–Re distance, pyrazolato ligands are able to change their bonding geometry, namely the Re–N distances and N–N–Re angles. For the former parameter there is no significant difference between the $\mu\text{-H}$ and $\mu\text{-OH}$ species (average 2.164 and 2.163 Å, respectively), while the bromide derivative shows an average value of 2.174 Å. More sensitive to the nature of the bridging group are the N–N–Re angles, which display a regular trend on moving from $\mu\text{-H}$ (115.5°) to $\mu\text{-OH}$ (120.0°) and $\mu\text{-Br}$ (124.6°). Another feature of the μ -pyrazolato coordination capabilities is the twist of the pz ring with respect to the Re–Re dumbbell. In **4**, the off-plane displacement of the rhenium atoms ranges from +0.050(5) (Re(1)) and –0.226(5) Å (Re(2)) with respect to pz(1–2) to +0.087(5) (Re(1)) and –0.076(5) Å (Re(2)) with respect to pz(3–4). Similar values have been observed in group 11 metal pyrazolates.^{15c}

In both **3a** and **4** the carbonyl ligands are linear with Re–C–O angles between 175.4(3)° and 179.7(3)°. All pyrazolato moieties in anions **3a** and **4** are planar within experimental errors, the maximum RMS out of plane deviation being 0.003 Å.

The N–H··· π -Electrons Hydrogen Bond. “Non-classic” hydrogen bond interactions involving π -electrons as an acceptor have been previously recognized and

(14) (a) Hanton, L. R.; Hunter, C. A.; Purvis, D. H. *J. Chem. Soc., Chem. Commun.* **1992**, 1134. (b) Allen, F. H.; Hoy, V. J.; Howard, J. A. K.; Thalladi, V. R.; Desiraju, G. R.; Wilson, C. C.; McIntyre, G. J. *J. Am. Chem. Soc.* **1997**, *119*, 3477.

(15) (a) Ardizzoia, A. G.; Angaroni, M. A.; La Monica, G.; Cariati, F.; Cenini, S.; Moret, M.; Masciocchi, N. *Inorg. Chem.* **1991**, *30*, 4347. (b) Ardizzoia, A. G.; Beccalli, E. M.; La Monica, G.; Masciocchi, N.; Moret, M. *Inorg. Chem.* **1992**, *31*, 2706. (c) Ardizzoia, A. G.; Cenini, S.; La Monica, G.; Masciocchi, N.; Moret, M. *Inorg. Chem.* **1994**, *33*, 1458.

(16) Nubel, P. O.; Wilson, S. R.; Brown, T. L. *Organometallics* **1983**, *2*, 515.

described (see for instance refs 14 and 17). To the best of our knowledge (substantiated by a thorough search through the October 1997 release of the Cambridge Crystallographic Database for similar intra and intermolecular interactions), there are no previous examples of structurally characterized hydrogen bonds involving compounds with the π -electrons of *nitrogen-heterocycles* as acceptors (while phenyl π -electrons are already known¹⁴) and N–H groups as donors.

The NMR data provide evidence that this intramolecular hydrogen bond is maintained in solution and features the dominant conformation in a noncoordinating solvent such as CH_2Cl_2 .

The N–H protonic resonance of **3a** is observed in CD_2Cl_2 at 193 K at δ 7.12 (δ 7.78 at 298 K), which is significantly upfield with respect to the range of values usually found in complexes containing terminally bonded Hpz (δ values between 12 and 9 ppm, at room temperature, in CDCl_3 or CD_2Cl_2).^{3c,17,18} In anion **6**, for instance, the N–H resonance is at δ 10.1 (CD_2Cl_2 , independent of the temperature). Inter- or intramolecular classical hydrogen bonds can move this signal at still higher frequencies, as observed for free pyrazole, involved in extensive intermolecular N–H \cdots N interactions. The high-field shift observed for **3a** is attributable to the shielding effect of the electronic π cloud of coordinated pyrazolate and, therefore, indicates that also in solution the N–H proton is pointing toward the center of the aromatic ring. In agreement with this, the species **3b**, which has been formulated as the anti isomer of **3a**, shows its NH resonance at a normal δ value (10.60 ppm) under the same conditions.

Indeed, the occurrence of an upfield shift has been previously used to reveal intermolecular π -hydrogen bonds, such as those between the C–H group of chloroform and the cyclopentadienyl rings of ferrocenes.¹⁹ Moreover, the shift at lower field undergone by the N–H resonance of pyrrole on dilution with an “innocent” solvent such as cyclohexane has also been attributed to a decrease of the intermolecular π -interactions between the N–H proton and the π -electron ring of a second molecule.²⁰ A similar shift, though considerably reduced in magnitude, was also observed for the α -CH protons of pyrrole. In anion **3a**, one of the ^1H NMR resonances of the C–H groups of pyrazole appears shifted upfield (δ 6.89 ppm, see Table 1) with respect to the typical values of pyrazole. On this basis, this signal could be attributed to the proton on the C atom α to NH (C3 in Figure 1), which is located at the periphery of the screening region of the π -electron density.

A 2D-NOESY experiment (Figure 3) at 298 K has confirmed this assignment. Indeed, the broad signal of the NH proton (δ 7.78) has two cross-peaks: one with

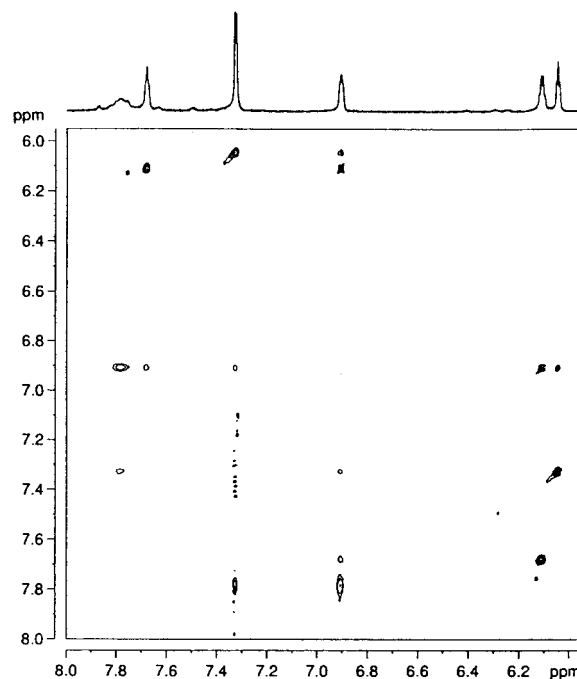


Figure 3. Contour plot of the negative levels of a ^1H 2D NOESY phase-sensitive experiment performed on a solution of $[\text{NEt}_4]\mathbf{3a}$ (298 K, CD_2Cl_2 , 7.05 T).

the α hydrogens of the pyrazolate moiety (at δ 7.33 ppm) and the other, stronger, with the signal at δ 6.91 ppm of the pyrazole. This last resonance displays strong through-space connectivities, also with the signals at 6.11 (H_β of Hpz) and 6.05 ppm (H_β of pz). Less intense correlations are observed with H_α of the pyrazole and with the signal at 7.68 ppm (H_γ of Hpz). The conformation observed in the solid state is, therefore, maintained in solution, even at room temperature.

The exoergonic nature of this H-bond interaction could be assumed as responsible for the dominance of the syn isomer **3a** over **3b**. An unconventional Os–H \cdots H–N interaction has been shown to stabilize the syn isomers of the $[\text{Os}_3\text{H}(\mu\text{-H})(\text{CO})_{10}\text{L}]$ complexes (L = $\text{NH}_2\text{-Et}$, NH_2Et_2).²¹ However, in the related $[\text{Re}_3(\mu\text{-H})_3(\mu\text{-}\eta^2\text{-NC}_5\text{H}_4)(\text{CO})_9(\text{NC}_5\text{H}_5)]^-$ anion, where H-bonding cannot occur, only the syn isomer was found.¹ Lower steric interligand repulsions could, therefore, be responsible in both cases for the syn configuration.

In the presence of a solvent able to act as an hydrogen-bond acceptor, such as acetone, intermolecular N–H \cdots solvent interactions replace the intramolecular H bond described above. The NMR data (see Table 1) indeed suggest that at low temperature in acetone anion **3a** adopts conformations in which the pyrazole ligand is hydrogen bound to the solvent. At 193 K, the NH resonance is now observed at δ 12.2, a value quite similar to that of free pyrazole in the same conditions (δ 12.94), thus showing the disappearance of the π -electron shielding effect and the involvement of NH in normal hydrogen bonds with acetone. The three resonances of the C–H's of the pyrazole occur at δ values close to those found in CD_2Cl_2 (see Table 1). However, in the present case, 1D NOE experiments (see Experimental Section) have shown that the positions of the

(17) (a) Atwood, J. L.; Hamada, F.; Robinson, K. D.; Orr, G. W.; Vincent, R. L. *Nature* **1991**, *349*, 683. (b) Cavaglioni, A.; Cini, R. *J. Chem. Soc., Dalton Trans.* **1997**, 1149. (c) Bakke, J. M.; Chadwick, D. *J. Acta Chem. Scand.* **1988**, *B42*, 223. (d) Kazaryan, S. G.; Lokshin, B. V.; Kimmel'fel'd, Y. M.; Materikova, R. B. *Izv. Akad. Nauk SSSR, Ser. Khim.* **1986**, *11*, 2603.

(18) (a) Alberte, B.; Sanchez Gonzalez, A.; Garcia, E.; Casas, J. S.; Sordo, J.; Castellano, E. E. *J. Organomet. Chem.* **1988**, *338*, 187. (b) Esteruelas, M. A.; Lahoz, F. J.; Lopez, A. M.; Onate, E.; Oro, L. A.; Ruiz, N.; Sola, E.; Tolosa, J. I. *Inorg. Chem.* **1996**, *35*, 7811.

(19) Cerichelli, G.; Illuminati, G.; Ortaggi, G.; Giuliani, A. M. *J. Organomet. Chem.* **1977**, *127*, 357.

(20) See Happe, J. A. *J. Phys. Chem.* **1961**, *65*, 72 and references therein.

(21) Aime, S.; Gobetto, R.; Valls, E. *Organometallics* **1997**, *16*, 5140.

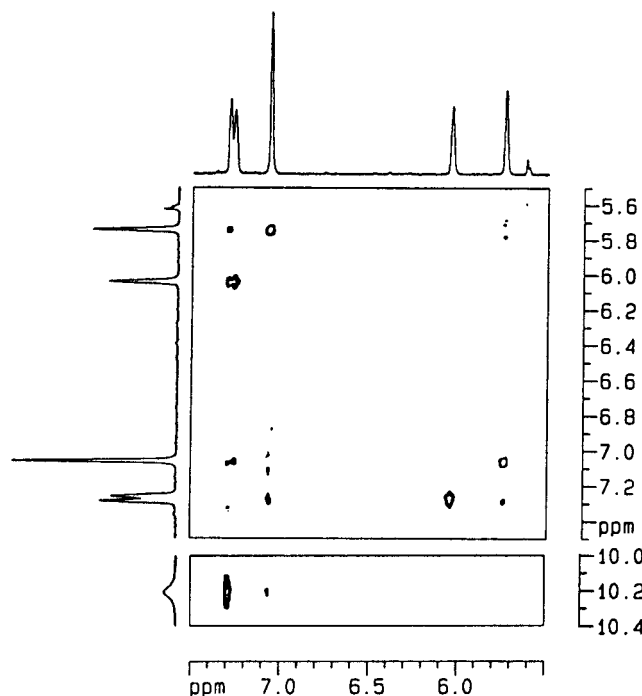
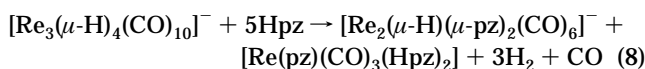


Figure 4. Contour plots of selected sections of a ^1H 2D NOESY phase-sensitive experiment performed on a solution of $[\text{NEt}_4]\mathbf{3a}$ (298 K, acetone- d_6 , 7.05 T). Only the negative levels have been plotted. The region of the CH pyrazolic resonances is shown in F2, while in F1 the sections of NH (bottom) and the CH pyrazolic resonances (top) are reported.

signals of H_α and H_γ are exchanged and the screening effect of the bridging pyrazolate ligand is now acting on H_γ while the resonance of H_α is at normal δ values. The pyrazole molecule is, therefore, rotated with respect to the conformation observed in CD_2Cl_2 .

On raising the temperature, the N–H signal of $\mathbf{3a}$ exhibits an upfield shift much higher than that observed for free pyrazole in the same conditions (see Table 1). The same behavior is observed for the signal of H_α , while that of H_γ undergoes a shift in the opposite direction (so that at room-temperature H_α and H_γ become almost isochronous, $\Delta\delta$ 0.05 ppm). These assignments have been confirmed by a 2D NOESY experiment at 298 K (Figure 4) that showed the correlation of the NH proton with the resonance at lower field (δ 7.30), thus assigned to H_α . This experiment has also shown that the $\text{H}_{\alpha,\gamma}$ protons of the bridging pyrazolate interact with three different protons of the terminal Hpz, namely H_α , H_γ , and NH. This indicates that different conformations are populated at room temperature and that they are in fast exchange. The δ values of the protonic resonances are, therefore, averaged values of the signals of the different conformers, and the shifts of the signals of H_α and H_γ with the temperature arise from the change of their relative populations.

Final Discussion. The overall reaction of $\mathbf{1}$ with pyrazole (eq 8) leads to fragmentation of the triangular cluster, with formal replacement of three hydrides by three pyrazolate anions. From this point of view, the

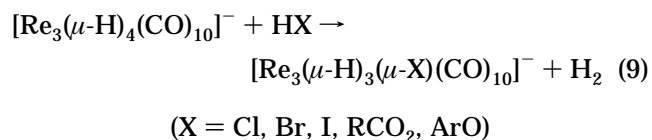


process is reminiscent of the reaction of $\mathbf{1}$ with I_2 or HI in nondonor solvents,²² which resulted in the stepwise fragmentation of the cluster skeleton by progressive substitution of the $\text{Re}(\mu\text{-H})\text{Re}$ interactions by $\text{Re}(\mu\text{-I})\text{-Re}$ ones. In particular, a dinuclear $[\text{Re}_2(\mu\text{-H})(\mu\text{-I})_2(\text{CO})_6]^-$ anion, similar to $\mathbf{4}$, was isolated and structurally characterized.

The reagents used in that case were strong electrophiles, able to attack the hydridic sites of the cluster anions, and the overall fragmentation occurred instantaneously, at room temperature, with stoichiometric amounts of reagents. In the present case, the amphoteric nature of pyrazole could suggest mechanisms based either on electrophilic or nucleophilic attack on $\mathbf{1}$. The drastic conditions (molten pyrazole as solvent) required even for the first reaction step (eq 1) could be in line either with the very low electrophilicity of pyrazole ($\text{p}K_a$ of the “pyrrolic” N–H bond 14.2)⁴ or with the poor propensity of $\mathbf{1}$ to react with nucleophiles, despite its electronic unsaturation.²³ The reaction with pyridine, for instance, at room temperature occurs at a reasonable rate only when the ligand is in large excess (typically when it is used as solvent).¹

Some clue is provided by the comparison of the rate of the reactions with Hpz of different 46-valence electron complexes $[\text{Re}_3(\mu\text{-H})_4(\text{CO})_9\text{L}]^-$. The increase of the rate in the order $\text{L} = \text{CO} < \text{PMe}_2\text{Ph} < \text{Hpz}$ corresponds to an increase of electron density on the cluster (and of “hydridic” character of the H ligands), on the basis of the known π -acceptor and σ -donor properties of the involved ligands. This, therefore, rules out that pyrazole coordination could be the rate-determining step and is in agreement with the idea of an electrophilic attack.

However, H_2 evolution from intermolecular $\text{pz-H}^{\delta+} - \text{H}^{\delta-} - \text{Re}$ interactions seems unlikely, due to the poor acidity of free Hpz. Reaction 9, in fact, has never been observed with acids weaker than phenol.²⁴ Moreover,



anion $\mathbf{6}$, in the absence of added ligands, is stable in solution for a few hours, despite possessing H ligands more hydridic than those of $\mathbf{1}$ and a pyrazole ligand more acidic than free Hpz (due to the coordination).

It seems, therefore, more likely that the $\text{H}^{\delta+} - \text{H}^{\delta-}$ interaction occurs concertedly with pyrazole coordination²⁵ or after this coordination, in a saturated (and therefore more electron rich) intermediate $\mathbf{11}$ of Scheme 3, containing a terminal hydride (more reactive) and a coordinated Hpz (more acidic). This intermediate could be formed (possibly in a fast preequilibrium step) not

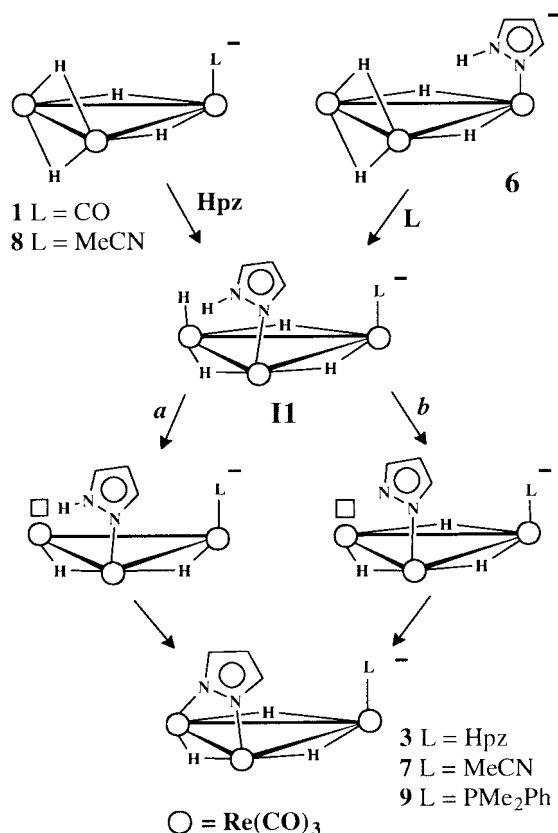
(22) Ciani, G.; D'Alfonso, G.; Romiti, P.; Sironi, A.; Freni, M. *Inorg. Chem.* **1983**, *22*, 3115.

(23) See, for instance: Beringhelli, T.; Ciani, G.; D'Alfonso, G.; Freni, M. *J. Organomet. Chem.* **1986**, *311*, C51.

(24) Beringhelli, T.; Ciani, G.; D'Alfonso, G.; Sironi, A.; Freni, M. *J. Chem. Soc., Dalton Trans.* **1985**, 1507.

(25) The concerted electrophilic/nucleophilic attack of HX acids on the μ_3 -imidoyl cluster $[\text{Os}_3(\mu\text{-H})(\mu_3\text{-}\eta^2\text{-C}=\text{NC}_3\text{H}_6)(\text{CO})_9]$ has been previously discussed. See: Gobetto, R.; Hardcastle, K.; Kabir, S. E.; Milone, L.; Nishimura, N.; Botta, M.; Rosenberg, E.; Yin, M. *Organometallics* **1995**, *14*, 3068.

Scheme 3



only by addition of pyrazole to a $[\text{Re}_3(\mu\text{-H})_4(\text{CO})_9\text{L}]^-$ complex, but also by addition of one L ligand to $[\text{Re}_3(\mu\text{-H})_4(\text{CO})_9(\text{Hpz})]^-$. The reaction of **6** with MeCN (eq 6) demonstrates the feasibility of this second route. The evolution of HD in the reaction of **6** with D-pz agrees with path b of Scheme 3, and it is reasonable to assume that the same mechanism is also operative for the other $[\text{Re}_3(\mu\text{-H})_4(\text{CO})_9\text{L}]^-$ complexes.

The formation of the pyrazolate anion in reactions 1, 4, 6, and 7 indicates that only the N–H bond is activated. Differently from what was observed in the addition of pyrazole on the $\text{Os}_3(\text{CO})_{10}$ fragment^{3c,7} or in the reaction of **1** with pyridine,¹ no species arising from the oxidative addition of the *ortho* C–H bond has been observed. This different behavior is easily rationalizable on the basis of Scheme 3. H_2 elimination from two hydrides of the intermediate **II** (path a) would give the H-unbridged Re–Re interaction, necessary in order to allow the competitive oxidative addition of N–H or C–H bonds. However, this does not occur because of the faster reaction between one hydride and the acidic H-pz proton.

The reaction of **1** with pyrazole shows, therefore, features intermediate between the reaction with pyridine (coordination of the basic nitrogen) and those with HX acids (H_2 elimination from oppositely polarized H atoms), in line with the amphiprotic nature of pyrazole.

This also confirms that rhenium hydrido–carbonyl cluster are less suitable than their isoelectronic osmium counterpart in activating C–H bonds, due to the presence of hydrogen bridges on the Re–Re interactions.

Experimental Section

The reactions were performed under N_2 , and solvents were dried and deoxygenated by standard methods. Pyrazole (Fluka) was used as received. Published methods were used for the syntheses of $[\text{NET}_4][\text{Re}_3(\mu\text{-H})_4(\text{CO})_{10}]^{13}$ and $[\text{NET}_4][\text{Re}_3\text{H}_4(\text{CO})_9]$.²⁶ The $[\text{Re}_3(\mu\text{-H})_4(\text{CO})_9(\text{Hpz})]^-$ and $[\text{Re}_3(\mu\text{-H})_4(\text{CO})_9(\text{PMe}_2\text{Ph})]^-$ anions were obtained quantitatively by treating $[\text{Re}_3\text{H}_4(\text{CO})_9]^-$ with the stoichiometric amount of the proper ligand. The NMR spectra were acquired on Bruker WP80, AC200, or DRX300 and Varian Gemini 200 spectrometers. Infrared spectra were obtained on a Perkin-Elmer 781 grating spectrophotometer or with a Bruker Vector 22 FT instrument.

Reactions of $[\text{NET}_4][\text{Re}_3(\mu\text{-H})_4(\text{CO})_{10}]$ ($[\text{NET}_4]\mathbf{1}$) with Pyrazole at 80 °C. Different Schlenk tubes containing the same amount of $[\text{NET}_4]\mathbf{1}$ (typically 8 mg, 0.008 mmol) and pyrazole (400 mg, 5.9 mmol), without any solvent, were maintained into a thermostat at 80 °C for different times. In each sample, pyrazole completely melted within about 1 min, giving yellow solutions. The reactions were quenched by introducing the samples into an ice bath. The gas-chromatographic analysis of the evolved gas showed the presence of H_2 and (at longer reaction times) CO. The addition of water gave a pale yellow precipitate, which was dried under vacuum. In the samples corresponding to the longer reaction times, treatment of the precipitate with *n*-hexane allowed the extraction of the neutral complex $[\text{Re}(\text{pz})(\text{CO})_3(\text{Hpz})_2]$ (**5**) (identified by its IR and NMR data).¹⁰ NMR analysis of the residue showed the presence of anions **2**, **3a**, and **4**, in different ratios. After 5 min, **2** was the main product (**2** 0.94, **3** 0.06), then its molar fraction slowly decreased (10 min, **2** 0.87; **3** 0.13) and the hydridic resonance of **4** appeared (30 min **2** 0.82, **3** 0.15, **4** 0.03; 60 min **2** 0.55, **3** 0.30, **4** 0.15; 120 min **2** 0.20, **3** 0.44, **4** 0.36). At very long reaction times, **4** became the main species (18 h **3** 0.58, **4** 0.42; 24 h **3** 0.35, **4** 0.65). Crystals of the $[\text{NET}_4]^+$ salt of anion **4** suitable for X-ray analysis were grown by slow diffusion of *n*-hexane into a concentrated CH_2Cl_2 solution. IR data: $[\text{NET}_4]\mathbf{2}$ (CH_2Cl_2) $\nu(\text{CO})$ 2098w, 2025m, 2006vs, 1985sh, 1943mw, 1910s(br) cm^{-1} ; $[\text{NET}_4]\mathbf{3a}$ (CH_2Cl_2) $\nu(\text{CO})$ 2034sh, 2005vs, 1992sh, 1912s cm^{-1} , $\nu(\text{N-H})$ 3340 cm^{-1} , $\Delta\nu_{1/2}$ 53 cm^{-1} (cfr. 3460 cm^{-1} , $\Delta\nu_{1/2}$ 27 cm^{-1} for free pyrazole in the same conditions, ca. 3×10^{-2} M); $[\text{NET}_4]\mathbf{4}$ (acetone) $\nu(\text{CO})$ 2019w, 2000s, 1992sh, 1898vs cm^{-1} . ¹H NMR data (acetone-*d*₆, 295 K): $[\text{NET}_4]\mathbf{2}$, δ 7.20 (d, 2, $\text{H}_{\alpha,\gamma}$, J_{HH} 2.0 Hz), 5.85 (t, 1, H_β , J_{HH} 2.0 Hz), –11.56 (s, 1), –13.59 (s, 2); $[\text{NET}_4]\mathbf{3a}$, δ 10.25 (s, 1, N–H), 7.30 (m, 1, H_α of Hpz), 7.25 (m, 1, H_γ of Hpz), 7.06 (m, 2, H_α of pz), 6.04 (m, 1, H_β of Hpz), 5.74 (m, 1, H_β of pz), –9.69 (s, 2), –11.16 (s, 1); $[\text{NET}_4]\mathbf{4}$, δ 7.30 (d, 4, $\text{H}_{\alpha,\gamma}$, J_{HH} 2.0 Hz), 5.86 (t, 2, H_β , J_{HH} 2.0 Hz), –8.50 (s, 1). Elemental analysis has been performed on a sample isolated after a reaction time of ca. 4 min and, therefore, was constituted mainly of $[\text{NET}_4]\mathbf{2}$ (contaminated by a very small amount of **3**). Anal. Calcd for $\text{C}_{21}\text{H}_{26}\text{N}_3\text{O}_{10}\text{Re}_3$: C, 24.3; H, 2.52; N, 4.04. Found: C, 24.4; H, 2.7; N, 4.5.

Reaction of $[\text{NET}_4]\mathbf{1}$ with D-pz at 80 °C. The vessels used for this experiment have been treated with D_2O and then maintained in an oven at 120 °C overnight. A sample of $[\text{NET}_4]\mathbf{1}$ (10.3 mg, 0.0106 mmol) was mixed without any solvent with D-pz (351 mg, 5.15 mmol, obtained by maintaining H-pz in 1 mL of D_2O for ca. 60 h). After 4 min at 80 °C, the reaction was quenched and the solid material was dissolved in THF. Addition of *n*-hexane caused the precipitation of a pale yellow solid, shown by NMR analysis to contain a mixture of unreacted **1** (about 42%), **2** (about 40%), and **3a** (about 17%). Comparison of the integrated intensities of the resonances in the hydridic and pyrazole regions indicated the occurrence of extensive deuteration (more than 50%) in the hydridic sites.

(26) Beringhelli, T.; D'Alfonso, G.; Garavaglia, M. G. *J. Chem. Soc., Dalton Trans.* **1996**, 1771.

This was confirmed by a ^2H NMR spectrum (acetone, 295 K), which showed substantially homogeneous deuteration in anions **1**, **2**, and **3a** and in the different hydridic sites.

Attempted Reaction of $[\text{NET}_4]_2$ with H_2 . A tube containing a CH_2Cl_2 solution of $[\text{NET}_4]_2$ (0.018 M) was maintained in an autoclave under 80 atm of H_2 at room temperature for 6 days. The solution was evaporated to dryness, and the residue, analyzed by NMR in deuteroacetone, was still the starting material.

Reaction of $[\text{NET}_4]_3\text{a}$ with CO. A solution of $[\text{NET}_4]_3\text{a}$ (12 mg, 0.0111 mmol) in THF (3 mL) was saturated with CO at 193 K. The sample was then maintained under CO atmosphere for 6 days. NMR analysis (acetone- d_6 , 298 K) of the residue showed the complete transformation of the starting material into the anion **2**.

Reaction of $[\text{PPh}_4][\text{Re}_3(\mu\text{-H})_4(\text{CO})_9(\text{Hpz})]$ ($[\text{PPh}_4]_6$) with Pyrazole at 298 K. A sample of $[\text{PPh}_4]_6$ (11.6 mg, 0.0101 mmol) was dissolved in CD_2Cl_2 (0.5 mL) in a NMR tube and treated with pyrazole (7.6 mg, 0.112 mmol). ^1H NMR spectra, acquired at different times, showed the clean transformation of **6** into **3a** and **3b**, as illustrated in Figures 1 of the Supporting Information. Due to the low concentration of **3b**, the large excess of free Hpz, and the presence of the PPh_4^+ cation, only four of the pyrazolic resonances of **3b** could be detected at δ 10.6 (1, NH), 7.12 (2, $\text{H}_{\alpha,\gamma}$ of pz), 6.14 (1, H_β of Hpz), and 5.80 (1, H_β of pz) ppm. The same reaction was also performed with D-pz, and NMR monitoring of the reaction showed the appearance of a *pseudotriplet*, centered at δ 4.4 ppm, attributable to HD (J_{HD} 43 Hz). Crystals of the $[\text{PPh}_4]^+$ salt of anion **3a** suitable for X-ray analysis were grown by slow diffusion of *n*-hexane into a concentrated CH_2Cl_2 solution. The elemental analysis performed on some of these crystals gave results in agreement with the presence of clathrated CH_2Cl_2 , revealed by the X-ray diffractometric investigation.

Reaction of $[\text{NET}_4]_6$ with CO. A sample of $[\text{NET}_4]_6$ (8.0 mg, 0.0078 mmol) was dissolved in CH_2Cl_2 (ca. 8 mL), and the solution was saturated with CO at room temperature. IR and NMR analyses, after 2.5 h, showed the quantitative formation of anion **1**.

Reaction of $[\text{NET}_4]_6$ with PMe_2Ph . A sample of $[\text{NET}_4]_6$ (12.3 mg, 0.012 mmol) in acetone- d_6 was treated with PMe_2Ph (1.5 μL , 0.0105 mmol) at 193 K. NMR spectra at 193 K showed the slow formation of the substitution derivative $[\text{Re}_3(\mu\text{-H})_4(\text{CO})_9(\text{PMe}_2\text{Ph})]^-$, which became quantitative when the temperature was raised to 298 K. NMR data of the product (acetone- d_6 , 298 K): δ 7.4–7.7 (m, 5, Ph), 1.86 (d, 6, Me, J_{PH} 8.0 Hz), –7.57 (d, 1, J_{PH} 6.1 Hz), –8.50 (d, 1, J_{PH} 2.9 Hz), –12.58 (d, 2, J_{PH} 17 Hz).

Reaction of $[\text{PPh}_4]_6$ with MeCN at 298 K. A sample of $[\text{PPh}_4]_6$ (11.3 mg, 0.0098 mmol) was dissolved in a NMR tube in CD_2Cl_2 and treated with MeCN (7.4 μL , 0.129 mmol). The sample was maintained at room temperature, and NMR spectra were acquired at different times, showing mainly the slow formation of the substitution derivative $[\text{Re}_3(\mu\text{-H})_4(\text{CO})_9(\text{NCMe})]^-$ (**8**) and of the novel species $[\text{Re}_3(\mu\text{-H})_3(\mu\text{-}\eta^2\text{-pz})(\text{CO})_9(\text{NCMe})]^-$ (**7**) (6 h ca. 80%, 17%, 2%, and 1% of **6**, **8**, **7**, and **3a**, respectively; 22 h 63%, 26%, 9%, and 2%; 48 h 42%, 34%, 22%, and 3%; 110 h 17%, 33%, 43%, and 7%). NMR data of **7** (CD_2Cl_2 , 298 K): δ 7.11 (d, 2, $\text{H}_{\alpha,\gamma}$, J_{HH} 1.9 Hz), 5.75 (t, 1, H_β , J_{HH} 1.9 Hz), 1.78 (s, 3, MeCN), –10.79 (s, 2, H_a), –11.66 (s, 1, H_b) ppm.

Reaction of $[\text{NET}_4][\text{Re}_3(\mu\text{-H})_4(\text{CO})_9(\text{PMe}_2\text{Ph})]$ with Hpz at 298 K. A sample of $[\text{NET}_4][\text{Re}_3(\mu\text{-H})_4(\text{CO})_9(\text{PMe}_2\text{Ph})]$ (15 mg, 0.014 mmol) was dissolved in CD_2Cl_2 in a NMR tube and treated with pyrazole (9.6 mg, 0.14 mmol). NMR monitoring showed the slow appearance of the hydridic resonances attributable to the novel anions $[\text{Re}_3(\mu\text{-H})_3(\mu\text{-}\eta^2\text{-pz})(\text{CO})_9(\text{PMe}_2\text{Ph})]^-$ (about 40% after 24 h) (**9a** and **9b**, 4:1 ratio). After 6 days, the conversion was complete. ^1H NMR data of the main product **9a** (CD_2Cl_2 , 298 K): δ 7.04 (d, 2H, $\text{H}_{\alpha,\gamma}$, J_{HH} 1.85 Hz), 5.81 (t, 1H, H_β , J_{HH} 1.85 Hz), 1.50 (d, 6H, Me, J_{HP} 9

Hz), –11.66 (d, 1H, J_{HP} 3.0 Hz), –11.98 (d, 2H, J_{HP} 18.6 Hz) ppm. ^1H NMR data of **9b** (CD_2Cl_2 , 298 K): δ 7.22 (d, 1H, $\text{H}_{\alpha,\gamma}$, J_{HH} 1.85 Hz), 7.20 (d, 1H, $\text{H}_{\alpha,\gamma}$, J_{HH} 1.85 Hz), 5.85 (t, 1H, H_β , J_{HH} 1.85 Hz), 2.13 (d, 6H, J_{HP} 9 Hz), –11.78 (s, 1H), –13.07 (d, 1H, J_{HP} 17.1 Hz), –13.30 (s, 1H) ppm.

Variable-Temperature Spectra and nOe Measurement of $[\text{NET}_4]_3\text{a}$. A sample of $[\text{NET}_4]_3\text{a}$ (19.1 mg, 0.018 mmols) was dissolved in acetone- d_6 (0.5 mL) into a NMR tube, and ^1H NMR variable-temperature spectra were acquired on a Bruker AC 200 spectrometer. The same sample was also used for nOe difference experiments performed at 193 K. Saturation radio-frequency fields have been applied for 300 ms on and off resonance with respect to the selected signal. The acquisitions have been cycled until a good signal-to-noise was achieved in the spectra obtained through the Fourier transform of the difference of the fids. Irradiation of the NH signal resulted in an enhancement of the signal at 7.64 ppm. When this last signal was irradiated, enhancements at 12.19 and 6.07 ppm were observed. Control experiments have been performed by irradiation of the signals at 6.07 and 6.61 ppm: positive nOe were observed at 7.64 and 6.61 ppm, and at 6.07 ppm respectively. A 2D-NOESY phase-sensitive²⁷ experiment was performed, in the same solvent, on a Bruker DRX 300 at 298 K using a mixing time of 2.0 s. Data points (1K) have been collected over a spectral width of 1800 Hz for each of the 40 transients. The data have been zero-filled twice to 1K in F_1 dimension and weighted with shifted sine bell functions before Fourier transform. A saturated solution of $[\text{NET}_4]_3\text{a}$ in CD_2Cl_2 was used for a 2D-NOESY experiment (Bruker DRX 300), performed at 298 K in the phase-sensitive mode using a mixing time of 2.2 s. There were 1K data points collected over a spectral width of 783 Hz for each of the 16 transients. The data have been zero-filled twice to 1K in F_1 dimension and weighted with shifted sine bell functions before Fourier transform.

X-ray Analysis of **3a and **4**.** (a) **Collection and Reduction of X-ray Data.** Suitable crystals of **3a** and **4** were mounted in air on a glass fiber tip and then onto a goniometer head. Table 2 contains the details of the crystal parameters and data collection and refinement procedures. Single-crystal X-ray diffraction data were collected on a Siemens SMART CCD three-circle area detector at –50 °C using graphite-monochromatized Mo K α radiation ($\lambda = 0.71073 \text{ \AA}$). Unit cell parameters and an orientation matrix were obtained from least-squares refinement on reflections measured in three different sets of 15 frames each in the range $0^\circ < \theta < 23^\circ$.

The intensity data were collected using the ω -scan technique within the limits $4^\circ < 2\theta < 56^\circ$. Approximately a full sphere of data was collected with the frame width set to 0.3° , the sample–detector distance fixed at 5.5 cm, and a detector exposition for each frame of 10 s. The first 100 frames were recollected at the end of collection to monitor crystal decay, which was not observed, thus no time-decay correction was needed. The collected frames were processed by SAINT software for integration; an absorption correction was applied together with merging (SADABS).

(b) **Solution and Structure Refinement.** The structures have been solved by direct methods (SIR92²⁸) and difference Fourier methods and subsequently refined by full-matrix least-squares against F_o^2 using all reflections and the program SHELXL97²⁹ on a Silicon Graphics Indigo computer. Scattering factors for neutral atoms and anomalous dispersion corrections were taken from the internal library of SHELXL97. All non-hydrogen atoms were given anisotropic displacement

(27) Bodenhausen, G.; Kogler, H.; Ernst, R. R. *J. Magn. Reson.* **1984**, *58*, 370.

(28) Altomare, A.; Casciaro, G.; Giacovazzo, C.; Guagliardi, A.; Burla, M. C.; Polidori, G.; Camalli, M., *J. Appl. Crystallogr.* **1994**, *27*, 435.

(29) Sheldrick, G. M. *SHELXL-97: program for structure refinement*; University of Göttingen: Göttingen, Germany, 1997.

parameters. Hydrogen atoms were first observed in a difference Fourier map and then included in idealized positions and refined riding on their parent atoms with isotropic displacement parameters of 1.2 times that of the pertinent atom.

Hydride positions were confirmed on the basis of the other ligands stereochemistry, and optimized coordinates were determined by means of HYDEX³⁰ with $d_{\text{Re-H}} = 1.85 \text{ \AA}$.

The CH_2Cl_2 clathrated molecules in **4** were found disordered with two-half molecules on a 2-fold axis (Wyckoff position 4e).

The final conventional agreement indexes are listed in Table 2. Selected bond parameters are reported in Table 3.

(30) Orpen, A. G. *J. Chem. Soc., Dalton Trans.* **1980**, 2509.

Acknowledgment. The authors warmly thank Mr. Pasquale Illiano for his accurate and skillful collaboration in the acquisition of the NMR data.

Supporting Information Available: Tables of X-ray analysis data, final atomic coordinates, anisotropic displacement parameters, full bond distances and angles, and least-squares planes and a figure concerning the reaction of $[\text{Re}_3(\mu\text{-H})_4(\text{CO})_9(\text{Hpz})]^-$ (**6**) with Hpz (17 pages). Ordering information is given on any current masthead page.

OM9800849